Appl. Phys. B (2015) 119:273–279
DOI 10.1007/s00340-015-6053-9

Applied Physics B
Lasers and Optics

A new method for the determination of optical band gap and the nature of optical transitions in semiconductors

Dariush Souri · Zahra Esmaeili Tahan

Received: 9 October 2014 / Accepted: 13 February 2015 / Published online: 26 February 2015

Abstract A new method (named as DASF: Derivation of absorption spectrum fitting) is proposed for the determination of optical band gap and the nature of optical transitions in semiconductors; this method only requires the measurement of the absorbance spectrum of the sample, avoiding any needs to film thickness or any other parameters. In this approach, starting from absorption spectrum fitting (ASF) procedure and by the first derivation of the absorbance spectrum, the optical band gap and then the type of optical transition can be determined without any presumption about the nature of transition. DASF method was employed on $(60-x)V_2O_5$–$40TeO_2$–xAg_2O glassy systems (hereafter named as TVAgx), in order to confirm the validity of this new method. For the present glasses, the DASF results were compared with the results of ASF procedure for, confirming a very good agreement between these approaches. These glasses were prepared by using the melt quenching and blowing methods to obtain bulk and film samples, respectively. Results show that the optical band gap variation for TVAgx glasses can be divided into two regions, $0 \leq x \leq 20$ and $20 \leq x \leq 40$ mol%. The optical band gap has a maximum value equal to 2.72 eV for $x = 40$ and the minimum value equal to 2.19 eV for $x = 40$. Also, some physical quantities such as the width of the band tails (Urbach energy), glass density, molar volume, and optical basicity were reported for the under studied glasses.

D. Souri (✉) · Z. E. Tahan
Department of Physics, Faculty of Science, Malayer University, Malayer, Iran
e-mail: d.souri@gmail.com; d.souri@malayeru.ac.ir

1 Introduction

Oxide and chalcogenide glasses have been studied extensively owing to some of their unique physical, optical, and semiconducting properties [1–24]. Nevertheless, of crystalline semiconductors, band gap determination in amorphous semiconductors is somewhat difficult because the edges of the tail states complicate the definition of the true optical band gap. Generally, three methods are frequently used to measure the absorption coefficient of thin films; one is to use the spectroscopic ellipsometer. Secondly, the Beer–Lambert's law is the one we can use to obtain absorption coefficient from the UV spectrophotometer. Thirdly, the absorption coefficient can be obtained by measuring transmittance (or absorbance) and thickness of the films. Whatsoever, the frequently used method of the band gap determination is based on measurement of the optical absorption coefficient and using the Tauc's method; this method has been extensively used for different binary and ternary semiconducting glasses [4, 6, 14, 25]. In Tauc's method, it is mandatory to measure the absorption coefficient (α) as a function of the incident photon wavelength; beside, as known, determination of absorption coefficient requires the measurement of the film absorbance, the reflectance, and the film thickness [26, 27]. In my recent works [28–30], I have used the absorption spectrum fitting method (ASF) [31] to obtain the band gap avoiding the film thickness measurement which commonly could not be measured precisely. In this procedure, band gap can be determined when only measurement of the film absorbance is available.

In the present work, starting from ASF procedure, a new method for the determination of optical band gap and the nature of optical transitions is proposed, which hereafter is called as derivation of absorption spectrum fitting method (DASF). As discussed in the next section, this procedure

has two characteristics: (a) as ASF, band gap can be determined when only measurement of the film absorbance or transmittance is available (any need to the film thickness is avoided) and (b) the optical band gap and the type of optical transition can be determined more precisely and more directly than Tauc's and ASF methods, avoiding any presumption about the type of optical transition. Finally, DASF method was employed for V_2O_5–TeO_2–Ag_2O glasses, and results were compared with the values obtained from ASF procedure on the same glasses, to identify the validity of the method; thus, the aims of this work are (1) Introducing the DASF procedure for determination of optical band gap and the nature of optical charge carrier transition, (2) employment of ASF method and also new DASF method on the V_2O_5–TeO_2–Ag_2O glasses and then comparing their results, (3) due to the importance of tellurate–vanadate glasses and also because of few reports on the physical and optical properties of the present glasses, we attempt to study and report the effect of Ag_2O on the optical and some physical quantities such as the width of the band tails (Urbach energy), glass density, molar volume, and optical basicity.

2 Theory of DASF method for the determination of optical band gap and the nature of optical charge carrier transitions

In order to achieve the optical band gap by using the proposed DASF method, we can begin with considering the ASF model at the absorption edge [28–31] as:

$$\alpha(\lambda) = B\,(hc)^{m-1}\,\lambda\left(\frac{1}{\lambda} - \frac{1}{\lambda_g}\right)^m \tag{1}$$

where $\alpha(\lambda)$ is the absorption coefficient defined by the Beer–Lambert's law as: $\alpha(\lambda) = (2.303/z)A$, considering z and A as film thickness and film absorbance, respectively, also, m is the index which can have different values 1/2, 3/2, 2, 3 [4, 14, 25]. λ_g, h, and c are wavelength corresponding to the optical gap($E_{gap}^{ASF} = hc/\lambda_g = 1239.83/\lambda_g$), Planck's constant and the velocity of the light, correspondingly. Using the Beer–Lambert's law, Eq. (1) can be rewrite as:

$$A(\lambda) = D\,\lambda\left(\frac{1}{\lambda} - \frac{1}{\lambda_g}\right)^m \tag{2}$$

where $D = [B(hc)^{m-1}z/2.303]$.

In ASF and Tauc's methods, one can determine m by examining the different m values and choosing the best fitted m value; so, using the optimized value of m, the optical gap can be obtained using the least squares technique.

In my proposed method (DASF), Eq. (2) can be written as:

$$\ln\left[\frac{A(\lambda)}{\lambda}\right] = \ln(D) + m\,\ln\left(\frac{1}{\lambda} - \frac{1}{\lambda_g}\right) \tag{3}$$

and then :

$$\frac{d\left\{\ln\left[A(\lambda)/\lambda\right]\right\}}{d(1/\lambda)} = \frac{m}{\left(\frac{1}{\lambda} - \frac{1}{\lambda_g}\right)} \tag{4}$$

Hence, upon Eq. (4), there should be a discontinuity in the $\frac{d\{\ln[A(\lambda)/\lambda]\}}{d(1/\lambda)}$ versus (1/λ) plot at$\frac{1}{\lambda} = \frac{1}{\lambda_g}$; by using the value of λ_g, optical band gap can be directly determined from $E_{gap}^{DASF} = 1239.83/\lambda_g$ in eV without any presumption of the nature of transition.

Now, using Eq. (3) and the λ_g value, obtained from the discontinuity at a particular energy gap, the value of m (indicating the nature of optical carrier transition) can be determined; therefore, the value of m can be obtained from the slope of the linear part of plot ln $[A(\lambda)/\lambda] - 1/\lambda$ plots. As described, this method helps us to (a) determine the optical band gap without any presumption of the nature of transition and (b) determine the m value (indicating the type of optical transition) using the obtained optical gap values for all the films.

2.1 Experimental procedure

Bulk and film samples of xAg_2O–$40TeO_2$–$(60-x)V_2O_5$ ternary glasses were prepared by normal melt quenching technique. Melting point of the obtained samples, hereafter termed as TVAgx glasses, was within the range of 660–730 °C, which shows increasing trend with increasing of Ag_2O component. To obtain bulk samples, the melt was poured on to a polished steel block and immediately pressed by another polished steel block, where the blocks were kept at room temperature. Bulk samples were annealed at 80 °C. To record the optical absorption spectra, amorphous layer samples were prepared using blowing procedure, by using a fine bore silica tube; because of insufficient viscosity, layer samples of TVAg50 were not formed and then its optical properties were not obtained. XRD patterns of the under studied samples were obtained by using a diffractometer (Unisantis-XMD-300, CuK_α, India). The density (ρ) of these samples was determined by the Archimedes's method using para-xylene (C_8H_{10}, density = 0.861 g/cm^3 at room temperature) as buoyant. The optical absorption/transmission spectra of the layers were obtained by using a UV–Visible double beam spectrophotometer (PerkinElmer, Lambda 25-USA) in the wavelength range 190–1100 nm at room temperature.

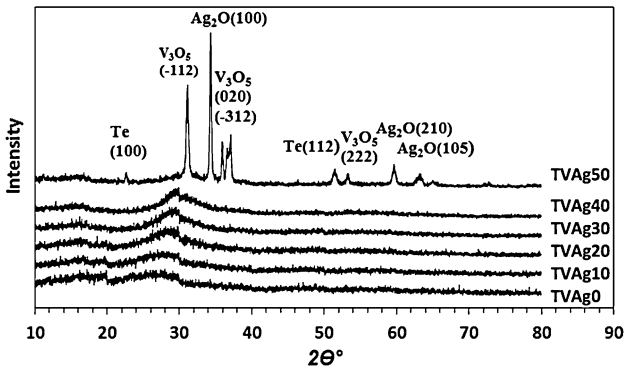

Fig. 1 XRD patterns of TVAgx glasses

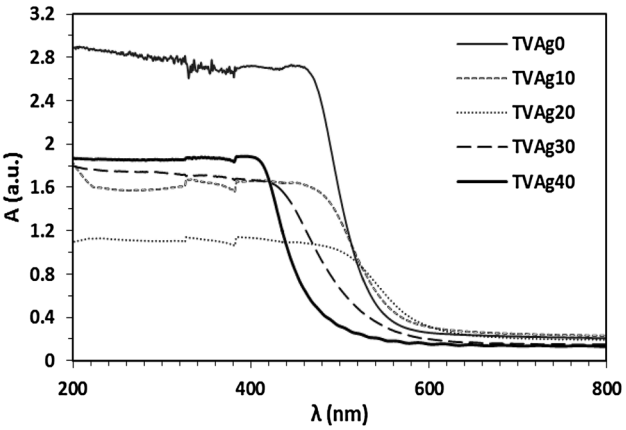

Fig. 2 Optical absorption spectra for TVAgx glasses

3 Results and discussion

3.1 XRD patterns

XRD patterns of TVAgx samples are shown in Fig. 1, confirming their glassy nature except for TVAg50. XRD peaks for TVAg50 are probably related to the microcrystalline phase of Ag–V in the amorphous matrix. One can attribute these peaks to the different structure of TVAg50 in comparison with other samples; in other word, it can be attributed to the structural changes resulting from the variation of the density of non-bridging oxygen's (NBOs), which can affect on the optical properties such as optical band gap, and width of the band tails. As mentioned before, XRD plots confirm the amorphous nature of the samples with $x < 50$ mol%; but for $x = 50$ mol%, some peaks could be seen. Observed peaks for TVAg50 are shown in Fig. 1. Upon XRD characterization, peaks at about $2\theta \approx 22.63°$ and 51.44° for TVAg50 matched with Te crystal phase. For this glass, the peaks observed at $2\theta \approx 31.11°$, 35.93°, 37.07°, 53.26°, and 64.99° matched with V_3O_5 crystal phase, correspond neither to those of starting powders, indicating that the crystallites of a complex nature are formed; also for TVAg50, peaks at $2\theta \approx 34.31°$, 59.66°, and 63.20° were probably (and not completely) matched with Ag_2O; it seems that the vanadium–silver (AgVO) phase are formed; also, for TVAg50, the crystalline peaks are due to the various transition of vanadium ions V^{2+}, V^{3+}, V^{4+}, and V^{5+}.

3.2 Optical and physical properties

3.2.1 Optical band gap and optical transition feature

In semiconductors, authors usually use the Tauc's formalism [27] and ASF [28, 31] method, but as mentioned in Sect. 1, we will use the proposed DASF method. The optical absorption spectra of all TVAgx samples are shown in Fig. 2.

In this work, we have performed both ASF and the new introduced DASF methods on the TVAgx glasses, which make us capable to compare their results and to justify the validity of DASF procedure. Upon the details of DASF method (in Sect. 2), the variation of $\frac{d\{\ln[A(\lambda)/\lambda]\}}{d(1/\lambda)}$ versus $(1/\lambda)$ was plotted for the present samples, as shown in Fig. 3; all curves show a discontinuity at $\frac{1}{\lambda} = \frac{1}{\lambda_g}$. By using the value of λ_g, optical band gap (in eV) can be determined using Eq. (5) as below:

$$E_{gap}^{DASF} = 1239.83/\lambda_g \tag{5}$$

Also, ASF plots of the present samples are shown in Fig. 4; in other word, in ASF method (Eq. 1), the variation of $(A/\lambda)^2$ versus $(1/\lambda)$ was plotted for the present samples, as shown in Fig. 4. By using the least squares technique, it was observed that the best fitting occurs for $m = 1/2$ (linear correlation coefficient: $R^2 = 0.9987$–0.9998), indicating the direct allowed band gap. For other values of m, R^2 was less than 0.9928. All obtained data of ASF and DASF methods on the present glasses are listed in Table 1.

Figure 5 shows the optical band gap values obtained by ASF and the proposed DASF procedure; in this figure, two aspects should be emphasized; Firstly, a good agreement can be seen between the values of the ASF gap obtained and those of DASF; in fact, the average deviation is up to 4 %; secondly, we know that in Tauc's and ASF methods, one have to identify the type of optical transition before the measurement of the band gap, but in DASF, any presumption of the nature of optical transition and also need to film thickness and least squares method are avoided.

Using the energy gap values, obtained from Fig. 3, the value of m can be determined (see Eq. 3). In better word, the value of m can be determined from the slope of the linear part of $\ln[A(\lambda)/\lambda]$ versus $1/\lambda$ plots. Plots of $\ln[A(\lambda)/\lambda]$ versus $1/\lambda$ are shown in Fig. 6. This method helps us to

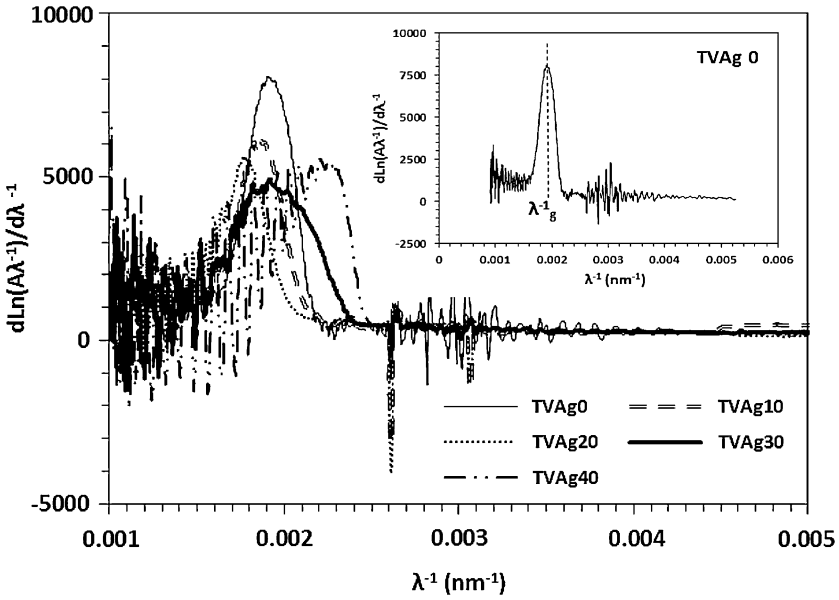

Fig. 3 Plot of d{ln(A/λ)}/d(1/λ) versus (1/λ) for a TVAgx glasses (DASF plots); as guide for eye, DASF plot of TVAg0 glass has been indicated as an inset in this figure. Discontinuity in DASF plot of TVAg0 is shown with dashed line, which indicates λ_g^{-1}

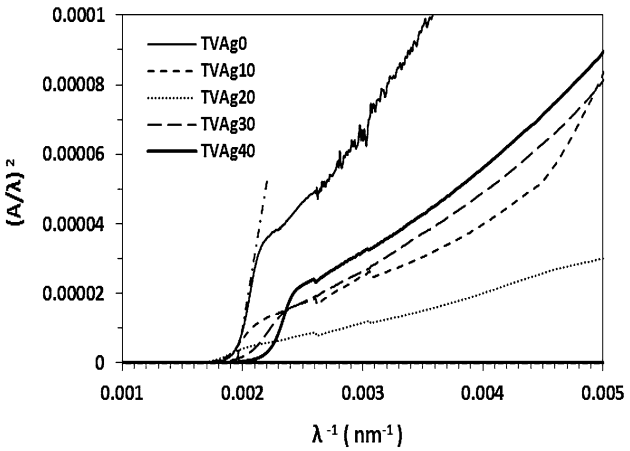

Fig. 4 ASF plots for TVAgx glasses. Least squared technique was used for the linear region of each curve; as guide for eye, typical linear part has been indicated for TVAg0 glass with dash-dotted line

calculate m values for all the film studied here without any presumption of the nature of transition. For TVAgx samples, the obtained m values varied in the range 0.483–0.869 and are almost about 1/2, which indicate direct allowed transition; this result is in good agreement with the optimum m value obtained from ASF for the present samples.

Finally, it should be noted that for many amorphous and crystalline semiconductors and also nanoparticle films, the absolute magnitude of the optical gap, as determined by the linear extrapolation in Tauc's and ASF procedures, is quite sensitive to the range over which the extrapolation is taken [28–31]; the proposed procedure avoids this problem since the complete spectrum is fitted.

It should be mentioned that in DASF method, the optical band gap decreases from 2.35 to 2.19 eV for $0 \leq x \leq 20$ and then increases to 2.72 eV for $20 \leq x \leq 40$.

This behavior may be associated with the structural changes occurring after the addition of Ag_2O. In other word, non-bridging oxygen (NBO) atoms are already present, and with the addition of Ag_2O ($0 \leq x \leq 20$) as a modifier, their concentration increases. Hence, the glass structure becomes less ordered, as can be justified by the E_{Tail} values (which will be presented in continue, see Table 1); addition of Ag_2O causes breaking of the regular structure of vanadium and tellurite (production of NBOs), leading to a decrease in the band gap [28–32]. This decreasing is due to an increase in the disorder and consequently the more extension of the localized states within the gap according to Mott and Davies [26]. On the other hand, energy band gap shows an increasing trend in $20 \leq x \leq 40$ region; it is suggested that this behavior is due to the structural modification that causes the decrease in non-bridging oxygen atoms, which can be justified by the decreasing trend in E_{Tail} (width of the tailing states in the gap).

For the better understanding, it is useful to discuss the tailing states in the band gap. In most amorphous semiconductors, fundamental absorption edge follows an exponential law [14, 27].

In ASF procedure, this exponential law is as below [28–31]:

$$A(\lambda) = D_1 \exp\left({}^{hc}/_{E_{Tail}\lambda}\right) \tag{6}$$

where D_1 is a constant, and E_{Tail} is width of the tail of localized states (Urbach energy) corresponding to the optical transition between localized tail states in adjacent of

Table 1 Data of ASF optical gap (E_{gap}^{ASF}), DASF optical gap (E_{gap}^{DASF}), the value of m (from ASF method) and the value of m (from DASF method), molar volume (V_M), density (ρ) and optical basicity (Λ_{th}) for TVAgx glasses; value of m indicates the type of optical transition

Glass	E_{gap}^{ASF} (eV)	E_{gap}^{DASF} (eV)	Value of m (from ASF method)	Value of m (from DASF method)	E_{Tail} (eV)	ρ (gr cm^{-3})	V_M (cm^3 mol^{-1})	Λ_{th}
TVAg0	2.41	2.35	1/2 : direct allowed transition	0.623: direct allowed transition	0.177	3.587	48.214	1.026
TVAg10	2.29	2.30	1/2: direct allowed transition	0.510: direct allowed transition	0.245	4.038	44.066	1.030
TVAg20	2.16	2.19	1/2: direct allowed transition	0.483: direct allowed transition	0.273	4.756	38.457	1.036
TVAg30	2.41	2.30	1/2: direct allowed transition	0.869: direct allowed transition	0.313	5.126	36.657	1.044
TVAg40	2.72	2.72	1/2: direct allowed transition	0.551: direct allowed transition	0.273	5.717	33.736	1.054
TVAg50	–	–	–	–	–	6.398	30.925	1.069

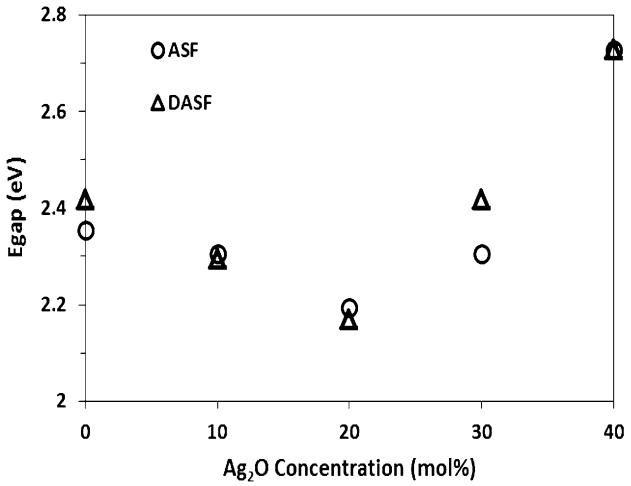

Fig. 5 Optical band gap determined by using ASF and proposed DASF procedures for TVAgx glasses; a good agreement can be seen between the values of the ASF gap obtained and those from DASF; in fact, the average deviation is up to 4 %

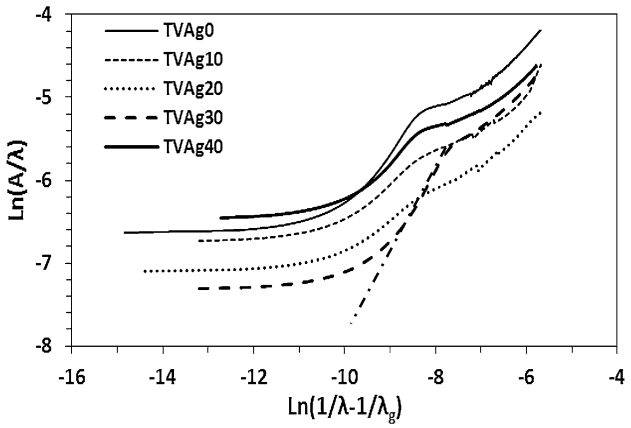

Fig. 6 Plot of ln(A/λ) versus ln(1/λ−1/λ_g) for TVAgx glasses (see Eq. 3). Values of 1/λ_g have been obtained from Fig. 3; as guide for eye, typical linear part has been indicated for TVAg30 glass with dash-dotted line

valence band and extended state in the conduction band lying above the mobility edge. Therefore, the values of E_{Tail}, in eV, can be obtained from the slope of the linear region of the ln (A) − (1/λ) curves using the equation E_{Tail} = 1239.83/slope; the least squares method (R^2 = 0.9982–0.9994) was employed to calculate the E_{Tail} values. Results of these calculations have been presented in Table 1 (see Fig. 7).

The values of the Urbach energy increase as the amount of Ag_2O increases (see Fig. 7; Table 1) for $0 \leq x \leq 30$ and decreases for x = 40. An increase in the Urbach energy can be considered being due to a higher number of defects or dangling bonds such as NBOs [33].

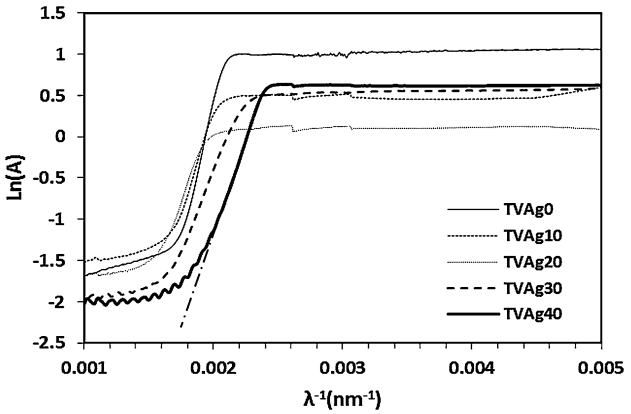

Fig. 7 Plot of ln(A/λ) versus (1/λ) for TVAgx glasses (Urbach curves: see Eq. 7). Least squared technique was used for the linear region of each curve; as guide for eye, typical linear part has been indicated for TVAg40 glass with dash-dotted line

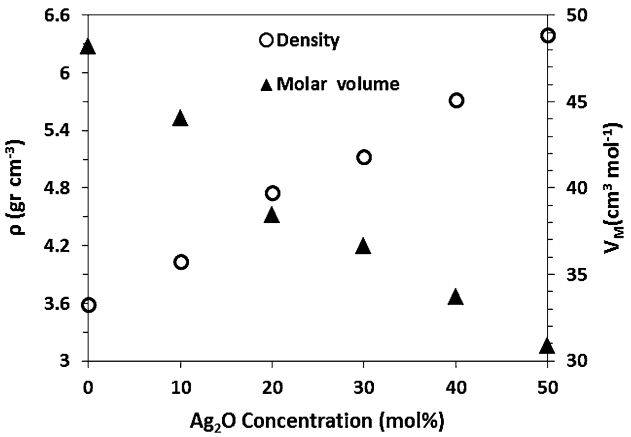

Fig. 8 Variation of the density and molar volume of TVAgx glasses with Ag_2O concentration

3.2.2 Density, molar volume, and optical basicity

The molar volume of a given composition can be calculated using the following formula:

$$V_m = \sum_i M_i/\rho \tag{7}$$

where M_i denotes the molar mass of the glass and $M_i = x_i A_i$. Here, x_i and A_i are the molar concentration and the molecular weight of the ith component, respectively.

Also, the theoretical optical basicity of each glass has been calculated by using the following expression [4, 34, 35]:

$$\Lambda_{\text{th}} == \sum_i x_i \Lambda_i \tag{8}$$

where x_i is the equivalent fraction of the constituent oxides, and Λ_i is its corresponding optical basicity. Here, the values of $\Lambda_{TeO_2} = 0.975$, $\Lambda_{V_2O_{5c}} = 1.04$, $\Lambda_{Ag_2O} = 1.25$ have been taken from the literature [34, 36].

The data of density and molar volume are presented in Table 1 and Fig. 8.

As mentioned before this, the dependence of density and molar volume of TVAgx glasses on Ag_2O amount is shown in Fig. 8. Generally, the density and the molar volume show opposite behavior, which is reasonable. In this work, the data of molar volume decrease as the content of Ag_2O increases and density increase as the content of Ag_2O increases. The variation in molar volume and density is the result of variation in atomic weight of glass system.

The variation of the optical basicity with addition of Ag_2O amount can be described in terms of change in the concentration of non-bridging oxygens and coordination number; in other word, this behavior may be explained knowing the role of Ag_2O as a modifier and the different structural units formed in these glasses. We know that increasing in optical basicity will result in decreasing of optical band gap. For the present glasses, in the $0 \leq x \leq 20$ region, this result can be observed; but, for $20 \leq x \leq 40$, nevertheless of increasing in optical basicity, optical band gap shows an increasing trend. It seems this behavior to be attributed to the structural changes of the samples, which can be observed from the XRD patterns; XRD patterns show the formation of an increasing intensity broad hump at about $2\Theta \sim 30°$ for $x \geq 20$, which finally result in crystalline peaks for TVAg50. Unfortunately, there are no reports about the structural characteristics of the present glasses; thus, for better and more detailed understanding of effect of Ag_2O addition in TVAgx glasses, it seems essential that the structural characterization to be investigated in future.

4 Conclusion

From the present work, the following points can be mentioned:

1. In this work, a new method (called as DASF) was proposed and described to easily and rapidly obtain the optical band gap and the nature of optical transitions in glasses. The main advantages of the DASF method are: (a) avoiding the film thickness measurement, (b) only measurement of the film absorbance is enough and (c) no any presumption of the nature of optical transition and no any need to linear extrapolation.
2. To evaluate the method, V_2O_5–TeO_2–Ag_2O glasses were analyzed. The values of the band gap obtained using ASF and DASF analysis methods were compared, and a good agreement between the values and similar trends was observed.
3. The optical band gap variation for TVAgx glasses can be divided into two regions, $0 \leq x \leq 20$ and

$20 \leq x \leq 40$ mol%. The DASF optical band gap has a maximum value equal to 2.72 eV for $x = 40$ and the value minimum equal to 2.19 eV for $x = 40$.

4. The Urbach energy is founded to be between 0.177 and 0.273 eV. Urbach energy shows an increasing trend in $0 \leq x \leq 30$ region and decreases for $x = 40$. In $0 \leq x \leq 30$ region, Urbach edge behavior is observed in these glasses, and the slope of the edge was founded to increase as the amount of Ag_2O increases.
5. The density depends on the composition: the greater the compactness of the structure the higher density. The density of the present samples increases with increase in Ag_2O amount.
6. The optical basicity of the fabricated glasses in the present work increases with increase in Ag_2O amount.

References

1. D. Souri, J. Phys. D Appl. Phys. **41**, 105102 (2008)
2. D. Souri, M. Elahi, Phys. Scr. **75**(2), 219–226 (2007)
3. D. Souri, M. Elahi, M.S. Yazdanpanah, Cent. Eur. J. Phys. **6**(2), 306–310 (2008)
4. D. Souri, S.A. Salehizadeh, J. Mater. Sci. **44**, 5800–5805 (2009)
5. B.V.R. Chowdari, P.P. Kumari, J. Phys. Chem. Solids **58**(3), 515–525 (1997)
6. M. Pal, K. Hirota, Y. Tsujigami, H. Sakata, J. Phys. D Appl. Phys. **34**, 459–464 (2001)
7. B.K. Sharma, D.C. Dube, A. Mansingh, J. Non-Cryst. Solids **65**, 39–51 (1984)
8. G.S. Murugan, Y. Ohishi, J. Non-Cryst. Solids **341**, 86–92 (2004)
9. S. Jayaseelan, P. Muralidharan, M. Venkateswarlu, N. Satyanarayana, Mater. Sci. Eng. B **118**, 136–143 (2005)
10. J. Lin, W. Huang, Z. Sun, C.S. Ray, D. Day, J. Non-Cryst. Solids **336**, 189–194 (2004)
11. S.V.G.V.A. Prasad, M.S. Reddy, N. Veeraiah, J. Phys. Chem. Solids **67**, 2478–2488 (2006)
12. A.A. El-Moneim, Mater. Chem. Phys. **73**, 318–322 (2002)
13. R.N. Sinclair, A.C. Wright, B. Bachra, Y.B. Dimitriev, V.V. Dimitriov, M.G. Arnaudov, J. Non-Cryst. Solids **232–234**, 38–43 (1998)
14. N. Chopra, A. Mansingh, G.K. Chadha, J. Non-Cryst. Solids **126**, 194–201 (1990)
15. A. Mansingh, V.K. Dhawan, J. Phys. C: Solid State Phys. **16**, 1675–1686 (1983)
16. S. Sakida, S. Hayakawa, T. Yoko, J. Phys.: Condens. Matter **12**, 2579–2595 (2000)
17. Y. Dimitriev, Y. Ivanova, M. Dimitrov, E.D. Lefterova, P.V. Angelov, J. Mater. Sci. Lett. **19**(17), 1513–1516 (2000)
18. M.M. El-Desoky, M.S. Al-Assiri, Mater. Sci. Eng. B **137**, 237–246 (2007)
19. P. Rozier, A. Burian, G.J. Cuello, J. Non-Cryst. Solids **351**, 632–639 (2005)
20. S. Szu, F. Chang, Solid State Ion. **176**, 2695–2699 (2005)
21. M.M. El-Desoky, J. Non-Cryst. Solids **351**, 3139–3146 (2005)
22. R. El-Mallawany, N. El-Khoshkhany, H. Afifi, Mater. Chem. Phys. **95**, 321–327 (2006)
23. V. Rajendran, N. Palanivelu, B.K. Chaudhuri, K. Goswami, J. Non- Cryst. Solids **320**, 195–209 (2003)
24. S. Gupta, A. Mansingh, Philos. Mag. Part B **78**(3), 265–277 (1998)
25. G. Turky, M. Dawy, Mater. Chem. Phys. **77**, 48–59 (2002)
26. N.F. Mott, E.A. Davis, *Electronic process in non-crystalline materials* (Clarendon Press, Oxford, 1979)
27. J. Tauc, A. Menth, J. Non- Cryst. Solids **8–10**, 569–585 (1972)
28. D. Souri, K. Shomalian, J. Non-Cryst. Solids **355**, 1597–1601 (2009)
29. D. Souri, Measurement **44**, 717–721 (2011)
30. D. Souri, M. Mohammadi, H. Zaliani, Electron. Mater. Lett. **10**(6), 1103–1108 (2014)
31. L.E. Alarcon, A. Arrieta, E. Camps, S. Muhl, S. Rudil, E.V. Santiago, Appl. Surf. Sci. **254**, 412–415 (2007)
32. S. Sindhu, S. Sanghi, A. Argawal, S.V.P. Sonam, N. Kishore, Phys. B **365**, 65 (2005)
33. R.P.S. Chakradar, G. Sivaramaiah, R. Lakshmana, N.O. Gopal, Spectrochim. Acta, Part A **62**, 761 (2005)
34. S. Sindu, S. Sanghi, A. Agarwal, V.P. Seth, N. Kishore, Mater. Chem. Phys. **90**, 83–89 (2005)
35. V. Dimitrov, T. Komatsu, J. Solid State Chem. **178**, 831–846 (2005)
36. A. Lebouteiller, P. Courtine, J. Solid State Chem. **137**, 94–103 (1998)